UCLouvain

LPHYS1303 - Finite differences project

The Double Pendulum

Solal Lemoine, Étienne Roger

January 2025

1 Introduction

A double pendulum system consists in a nutshell in a single pendulum hanging at the bottom of another single pendulum. In our case, we consider two dimensionless objects of mass resp. m_1 and m_2, each object being attached to a rod of fixed length resp. l_1 and l_2. We will restrict ourselves to the two-dimensional case.

This system is known to be a ***chaotic*** one, meaning that the dynamics of the objects, entirely determined by the angles θ_1 and θ_2, are very sensitive to the initial conditions (which are the initial values for θ_1,θ_2,$\dot{\theta}_1$,$\dot{\theta}_2$).

In this project, we will simulate the double pendulum system through a numerical model coded in python, and analyse its chaoticity for the simple case where $m_1 = m_2$ and $l_1 = l_2$. This analysis will be done mainly through a discussion about the **Lyapunov exponents** of the system (further details in the section 6).

2 Mathematical model

The simplest way to mathematically solve the system's dynamics is through **Lagrangian mechanics**.

The Lagrangian function characterizing the system is:

$$\begin{aligned} L = \frac{1}{2}\left(m_1+m_2\right) l_1^2\dot{\theta}_1^2 + \frac{1}{2}m_2 l_2^2\dot{\theta}_2^2 + m_2 l_1 l_2 \dot{\theta}_1\dot{\theta}_2\cos\left(\theta_1-\theta_2\right) \\ + \left(m_1+m_2\right) g l_1 \cos\theta_1 + m_2 g l_2 \cos\theta_2 \,. \end{aligned} \tag{2.1}$$

Hence the two **Euler-Lagrange equations** derived from it are:

$$\begin{aligned} \left(m_1+m_2\right) l_1\ddot{\theta}_1 + m_2 l_2\ddot{\theta}_2\cos\left(\theta_1-\theta_2\right) + m_2 l_2\dot{\theta}_2^2\sin\left(\theta_1-\theta_2\right) + g\left(m_1+m_2\right)\sin\theta_1 = 0 \\ m_2 l_2\ddot{\theta}_2 + m_2 l_1\ddot{\theta}_1\cos\left(\theta_1-\theta_2\right) - m_2 l_1\dot{\theta}_1^2\sin\left(\theta_1-\theta_2\right) + m_2 g\sin\theta_2 = 0 \end{aligned} \tag{2.2}$$

Isolating $\ddot{\theta}_1$ and $\ddot{\theta}_2$ gives the following two (still) coupled equations:

$$\begin{aligned} \ddot{\theta}_1 &= \frac{-g\left(2m_1+m_2\right)\sin\theta_1 - m_2 g\sin\left(\theta_1-2\theta_2\right) - 2\sin\left(\theta_1-\theta_2\right) m_2\left(\dot{\theta}_2^2 l_2 + \dot{\theta}_1^2 l_1\cos\left(\theta_1-\theta_2\right)\right)}{l_1\left(2m_1+m_2-m_2\cos\left(2\theta_1-2\theta_2\right)\right)} \\ \ddot{\theta}_2 &= \frac{2\sin\left(\theta_1-\theta_2\right)\left(\dot{\theta}_2^2 l_1\left(m_1+m_2\right) + g\left(m_1+m_2\right)\cos\theta_1 + \dot{\theta}_2^2 l_2 m_2\cos\left(\theta_1-\theta_2\right)\right)}{l_2\left(2m_1+m_2-m_2\cos\left(2\theta_1-2\theta_2\right)\right)} \end{aligned} \tag{2.3}$$

We can finally uncouple these two second-order equations into a set of **four first-order equations**, by defining the new variables ω_1 and ω_2 (this will be useful later for the numerical implementation):

$$\begin{aligned} \dot{\theta}_1 &= \omega_1 \\ \dot{\theta}_2 &= \omega_2 \\ \dot{\omega}_1 &= \frac{-g\left(2m_1+m_2\right)\sin\theta_1 - m_2 g\sin\left(\theta_1-2\theta_2\right) - 2\sin\left(\theta_1-\theta_2\right) m_2\left(\omega_2^2 L_2 + \omega_1^2 l_1\cos\left(\theta_1-\theta_2\right)\right)}{l_1\left(2m_1+m_2-m_2\cos\left(2\theta_1-2\theta_2\right)\right)} \\ \dot{\omega}_2 &= \frac{2\sin\left(\theta_1-\theta_2\right)\left(\omega_1^2 l_1\left(m_1+m_2\right) + g\left(m_1+m_2\right)\cos\theta_1 + \omega_2^2 l_2 m_2\cos\left(\theta_1-\theta_2\right)\right)}{l_2\left(2m_1+m_2-m_2\cos\left(2\theta_1-2\theta_2\right)\right)} \end{aligned} \tag{2.4}$$

No closed form solution for θ_1 and θ_2 are known, therefore the system can only be solved numerically.

3 Numerical implementation

We have four ordinary differential equations, all of the first order, that we will implement numerically via the finite differences method.

We will choose the **Runge-Kutta 4** scheme in this case, mainly for its simplicity (explicit scheme, no additional calculations needed compared to what has been done in 2).

Normally, we would want to use a *symplectic* scheme that can conserve the value of the system's total energy (which the RK4 scheme cannot). However, the error in the value of the energy created by a non-symplectic scheme is not significant enough for small timescales used to study a typical double pendulum ($\sim 10^2 s$). This will be clearly shown and explained in the section 5.

3.1 Runge-Kutta 4 scheme

The Runge-Kutta 4 scheme can be implemented as following in Python.

Runge-Kutta 4

```
def solve_RK4(f, u0, h, t_max):
    N = int(np.floor(t_max / h)) + 1    # Timesteps
    t = np.linspace(0, t_max, N)    # Time array
    u = np.zeros((N,4))    # Array containing theta_1, theta_2, omega_1 and omega_2
    u[0] = u0    # Imposing initial conditions
    for i in range(N - 1):
        k1 = h * f(u[i][0], u[i][1], u[i][2], u[i][3])
        k2 = h * f(u[i][0] + k1[0]/2, u[i][1] + k1[1]/2, u[i][2] + k1[2]/2, u[i][3] +
        ↪  k1[3]/2)
        k3 = h * f(u[i][0] + k2[0]/2, u[i][1] + k2[1]/2, u[i][2] + k2[2]/2, u[i][3] +
        ↪  k2[3]/2)
        k4 = h * f(u[i][0] + k3[0], u[i][1] + k3[1], u[i][2] + k3[2], u[i][3] + k3[3])
        u[i+1] = u[i] + 1/6 * (k1 + 2*k2 + 2*k3 + k4)
    return t, u
```

For our case, the `f` argument to the `solve_RK4` function has to be a four-dimensional array containing the derivatives of ω_1, ω_2, θ_1 and θ_2, which we already calculated in 2.4.

4 Visualisation of the system

An intuitive way to understand the "chaotic" behaviour of the system is through visual representations and graphs.

We can first of all plot the solutions to the system, i.e. ω_1, ω_2, θ_1 and θ_2, all with respect to the elapsed time.

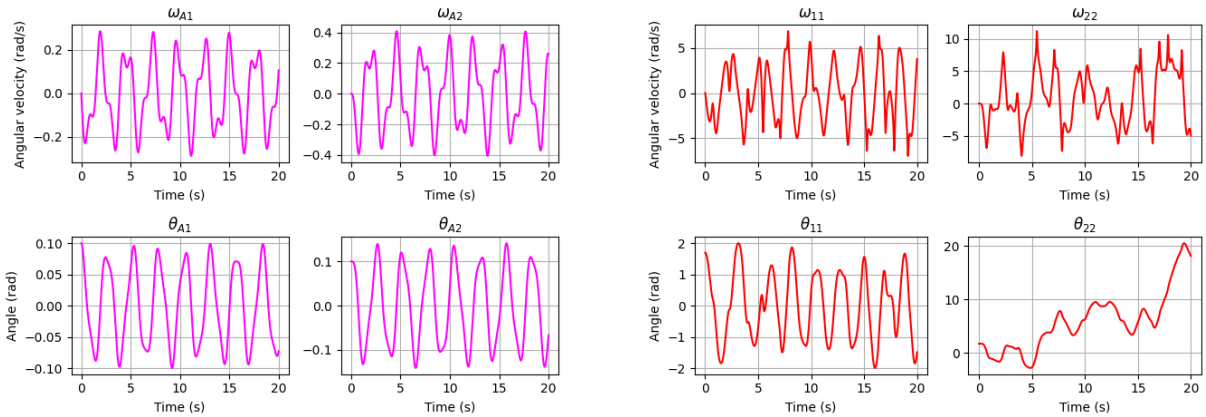

(a) Initial angles $\theta_1 = \theta_2 = 0.1$ rad

(b) Initial angles $\theta_1 = \theta_2 = 1.7$ rad

Figure 1

The graphs in figure 1 are not the most intuitive ones to understand what is really happening. At best,

we can know from the bottom right plots in figure 1a and 1b that the bottom mass (m_2) is behaving in a pseudo-oscillatory and chaotic manner, respectively.

A second way to highlight the nature of the system's behaviour is to compare the two angles at any given time t through a parametric plot. If the system is chaotic, the graph will resemble to that of a Brownian motion (fig. 2a), and if it is pseudo-oscillatory, it will present a regular pattern of some sort (fig. 2b).

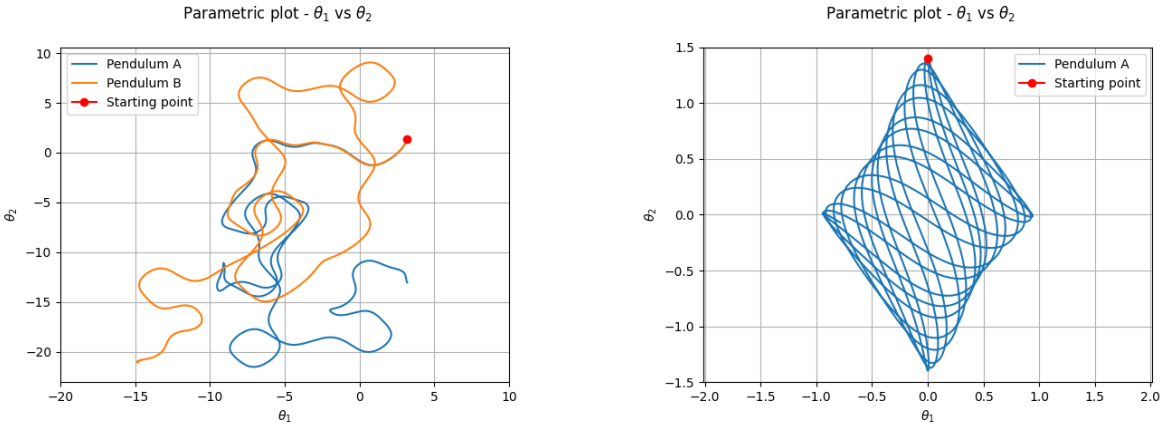

(a) Chaotic

(b) Pseudo-oscillatory

Figure 2

Obviously, an animation is the most intuitive way to visualise the system's behaviour. Although it is not possible to show one here, a couple of .gif files are available in our Gihub repository, such as chaotic.gif, which shows the motions of four pendula starting at once from almost identical initial conditions.

5 Energy of the system

As mentioned in section 3, the Runge-Kutta 4 scheme is not symplectic. This means that some energy is lost (or created) during the simulation of the system. We can see in figure 3 the energy loss, across 100 seconds of simulation, for each of four pendula, with initial conditions varying from 1.3 to 1.6 radians. Even after 100 seconds, the energy loss does generally not surpass 6%, which is fairly acceptable for a non-symplectic scheme.

We can also see that the more chaotic the movement, the more energy is lost. In figure 3, the pink line represents a pendulum[1] that is under the critical threshold for chaoticity, while the other three represent pendula that follow chaotic movements.

Note that the actual things that cause those spikes in energy loss are the sudden movements that cause the whole pendulum to swing widely in a short instant. Those kind of jerky movements do not occur when the initial conditions are low in energy, hence the better stability in energy for those less-chaotic systems.

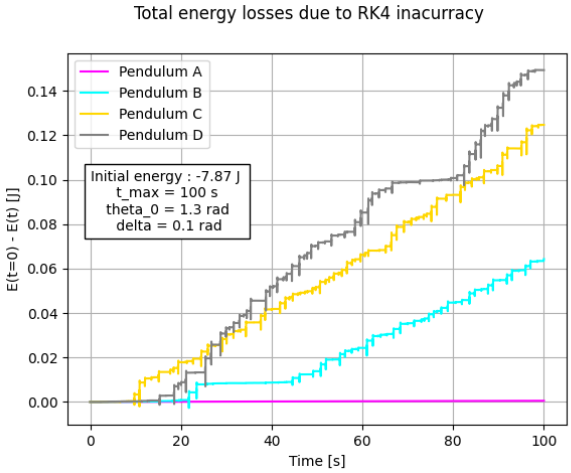

Figure 3: Energy loss for four pendula

[1]By "pendulum" we always mean "double pendulum" in this report.

6 Largest Lyapunov exponent

To analyse the chaoticity of the double pendulum system, we can compute the *largest Lyapunov exponent* λ_{max} characterizing the dynamical system.

To define it, we first consider two trajectories separated by a distance $\delta\mathbf{x}(t)$, with $\delta\mathbf{x}(0)$ very small. We can then find the time evolution of the distance thanks to the linear tangent operator $\mathbf{J}(x,t)$:

$$\frac{d\,\delta\mathbf{x}}{dt} = \mathbf{J}(\mathbf{x},t)\delta\mathbf{x} \tag{6.1}$$

The largest Lyapunov exponent can then be computed as

$$\lambda_{\max} = \lim_{t\to+\infty} \frac{1}{t} \ln\left(\frac{|\delta\mathbf{x}(t)|}{|\delta\mathbf{x}(0)|}\right) \tag{6.2}$$

There is in fact another way of determining λ_{max} : it is equal to the *maximum value of the real parts of the eigenvalues of the tangent linear operator* $\mathbf{J}(x,t)$.

While we understood that the main point for this project was to study the results produced by the "$\delta\mathbf{x}(t)$ method" eventually using eq.6.2, we have sometimes used the better accuracy of the "eigenvalue method" to our advantage by comparing our numerical results with those theoretical[2] ones.

Throughout our study, we have concluded that, if for a given initial condition $u(t=0)$ we get a λ_{max} very close to zero and seemingly tending to zero (although remaining positive), the system is considered as a non-chaotic one. If on the contrary, λ_{max} tends to a positive non-zero value, this would be a chaotic system.

6.1 Spin-up phase

By evaluating the lyapunov exponent at each time t, we clearly see that it converges whatever the initial condition (small or big initial energy). It tends to 0 if the system is locally non-chaotic (like in 4a) and to a constant greater than 0 if it is locally chaotic (like in 4b). We will call this asymptotical value the ***local largest lyapunov exponent***, or more simply ***local λ_{max}***.

To proceed with the "$\delta\mathbf{x}(t)$ method", both RK4 and the straightforward matrix exponential resolution have been tested to reproduce the time evolution of $\delta\mathbf{x}$, and both seem to be fairly equivalent in terms of accuracy[3]. Both methods can also be seen to approximate well enough for a large t the theoretical value of λ_{max}.

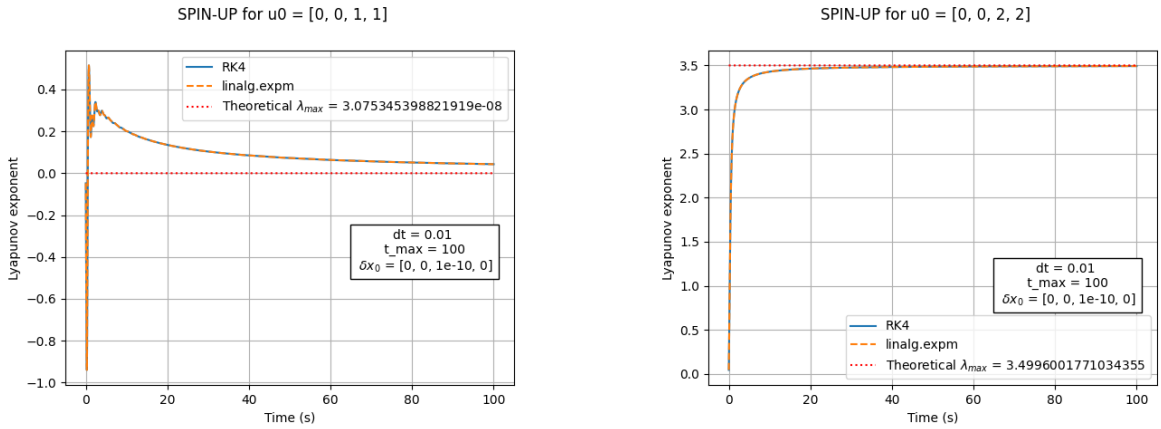

(a) Locally non-chaotic

(b) Locally chaotic

Figure 4

6.2 Local largest Lyapunov exponent

To better understand the tendencies in local λ_{max} values, the following plots have been produced. Figure 5a shows local λ_{max} evaluated at $t=20$, $t=100$, their average between those two moments (after filtering infinite or NaN values), and the theoretical value, all with respect to angle $\theta \in [0,\pi]$, when the initial condition of the pendulum is $u(t=0) = (\omega_1 = 0, \omega_2 = 0, \theta_1 = \theta, \theta_2 = \theta)$. We can observe here that there is a critical angle at which the local λ_{max} does not tend to zero anymore. This angle seems to be $\theta = \frac{\pi}{2}$.

[2] We will refer to the value of λ_{max} computed with the eigenvalue method as the "theoretical" λ_{max} from further on.

[3] It was however noted during our trial and errors that any timestep dt greater than 0.1 creates a constant bias in the computed λ_{max}

In figure 5b, we take a more general case of an arbitrary initial condition (while both initial angular velocities are kept null). We can see on the upper half of the secondary diagonal what figure 5a showed us: the exact spot where dark blue turns into green is where the flip occurs ($\theta_1 = \theta_2 = \frac{\pi}{2}$).

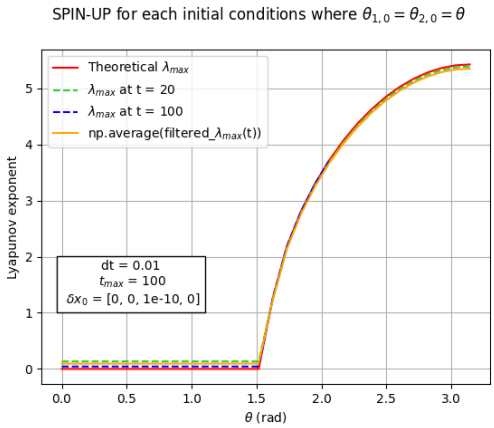

(a) Local λ_{max} vs initial angle θ

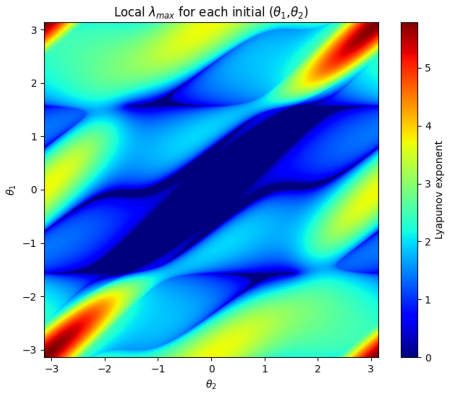

(b) Local theoretical λ_{max} for any initial (θ_1, θ_2)

Figure 5

6.3 Global largest Lyapunov exponent

The ***global largest Lyapunov exponent*** is the average of the local largest exponents evaluated many times on the trajectory of the pendulum, for a given initial condition. By doing this, we can judge more accurately if the initial condition is chaotic or not. For example, even though the local λ_{max} for initial position $u(t = 0) = (0, 0, \frac{\pi}{2}, \frac{\pi}{2})$ tended to be 0 (locally non-chaotic), we clearly see on figure 6a that this initial condition actually leads to chaotic dynamics.

We can then once again take the general case and plot the global λ_{max} for an arbitrary initial condition, as shown in figure 7a. The energy is seen to play a big role in the determination of the value of λ_{max}, for general tendencies seem to be conserved when compared to 7b. However, it is not the only important parameter: for values of θ_1 slightly bigger than θ_2, represented in the blue spike-like structure in figure 7a, the system stays non-chaotic, even for relatively high energy values. This is why we concluded that the initial condition plays also a key-role on the chaoticity of the double pendulum system, in addition to its energy.

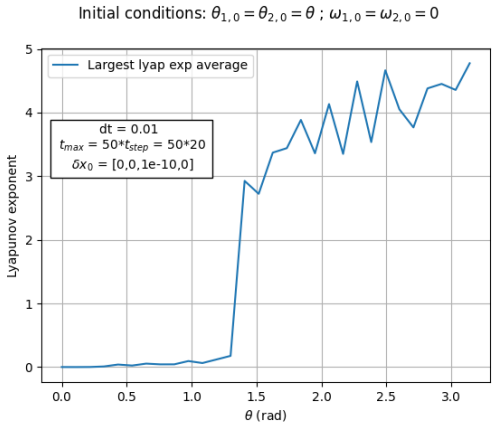

(a) Global λ_{max} for initial angles (θ, θ)

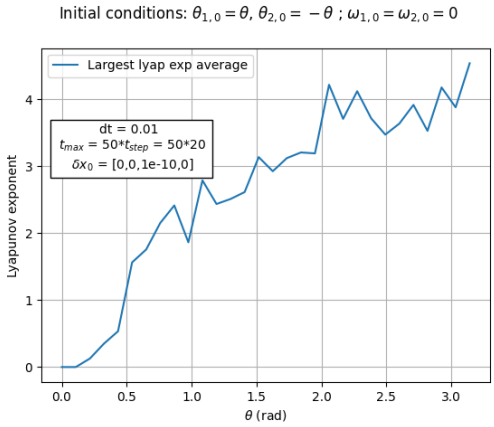

(b) Global λ_{max} for initial angles $(\theta, -\theta)$

Figure 6

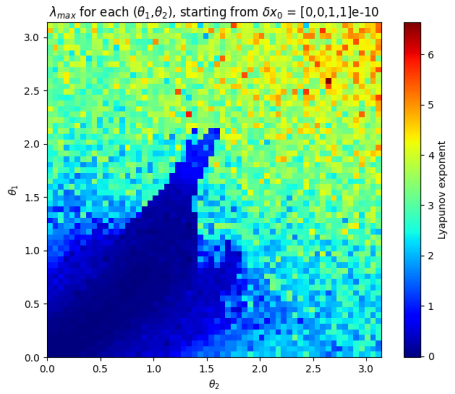

(a) Global λ_{max} for any initial angle pair (θ_1, θ_2)

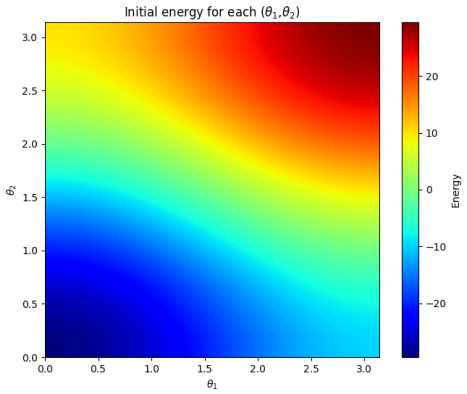

(b) Initial energy for comparison

Figure 7

7 Conclusion about chaoticity

Plots on figure 8 shows the paths followed by each mass in Cartesian coordinates for 100 seconds, for four almost identical (but each slightly different by +0.001 rad) initial conditions where $u(t = 0) = (\omega_1 = 0, \omega_2 = 0, \theta_1 = \theta, \theta_2 = \theta)$. We can visually and intuitively see a critical angle, seemingly between 1.381 and 1.382 rad(which matches with the largest lyapunov exponent prediction as visible in figure 6a), from which the system becomes chaotic. An even clearer visual representation of this critical angle for these exact initial conditions can be seen in action as an animation here.

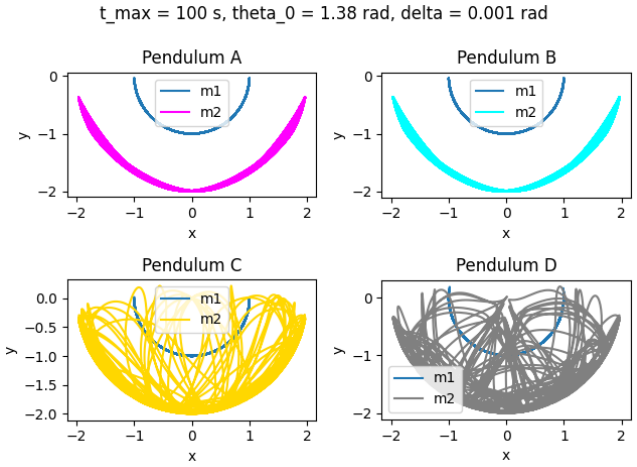

Figure 8: Paths followed by pendula starting near critical angle

Github repository

For further details on the used codes and produced graphics for this project, see our Github repository.